DARK MATTER

ASTR 333/433

TODAY

HYDRO SIMULATIONS
BARS & SPIRAL STRUCTURE
THIN & THICK DISKS
GALAXY MERGERS
TIDAL DWARFS

Homework 2
Due Now

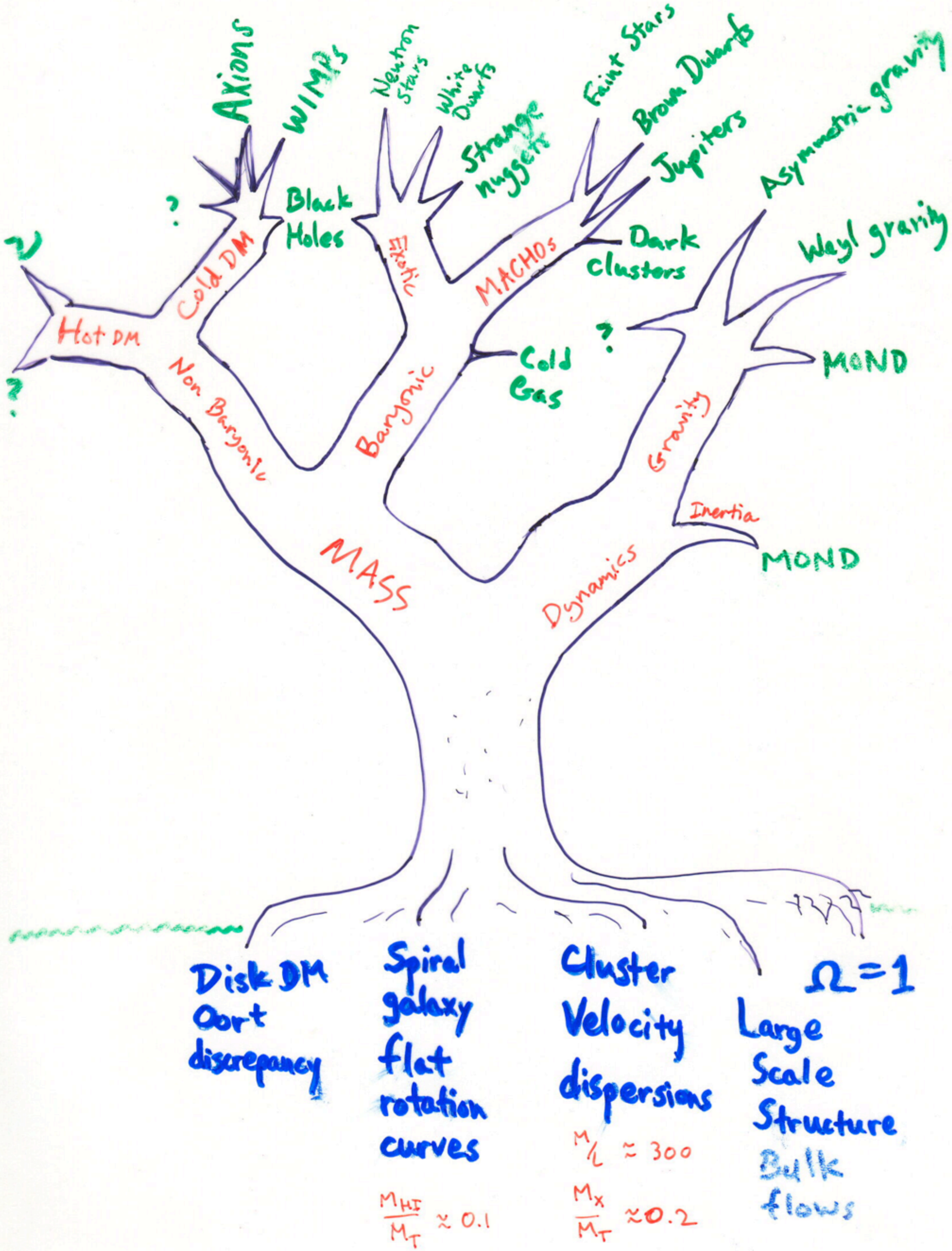

Kitchen sink cosmological models

Somerville & Dave 2015 ARA&A, 53, 51

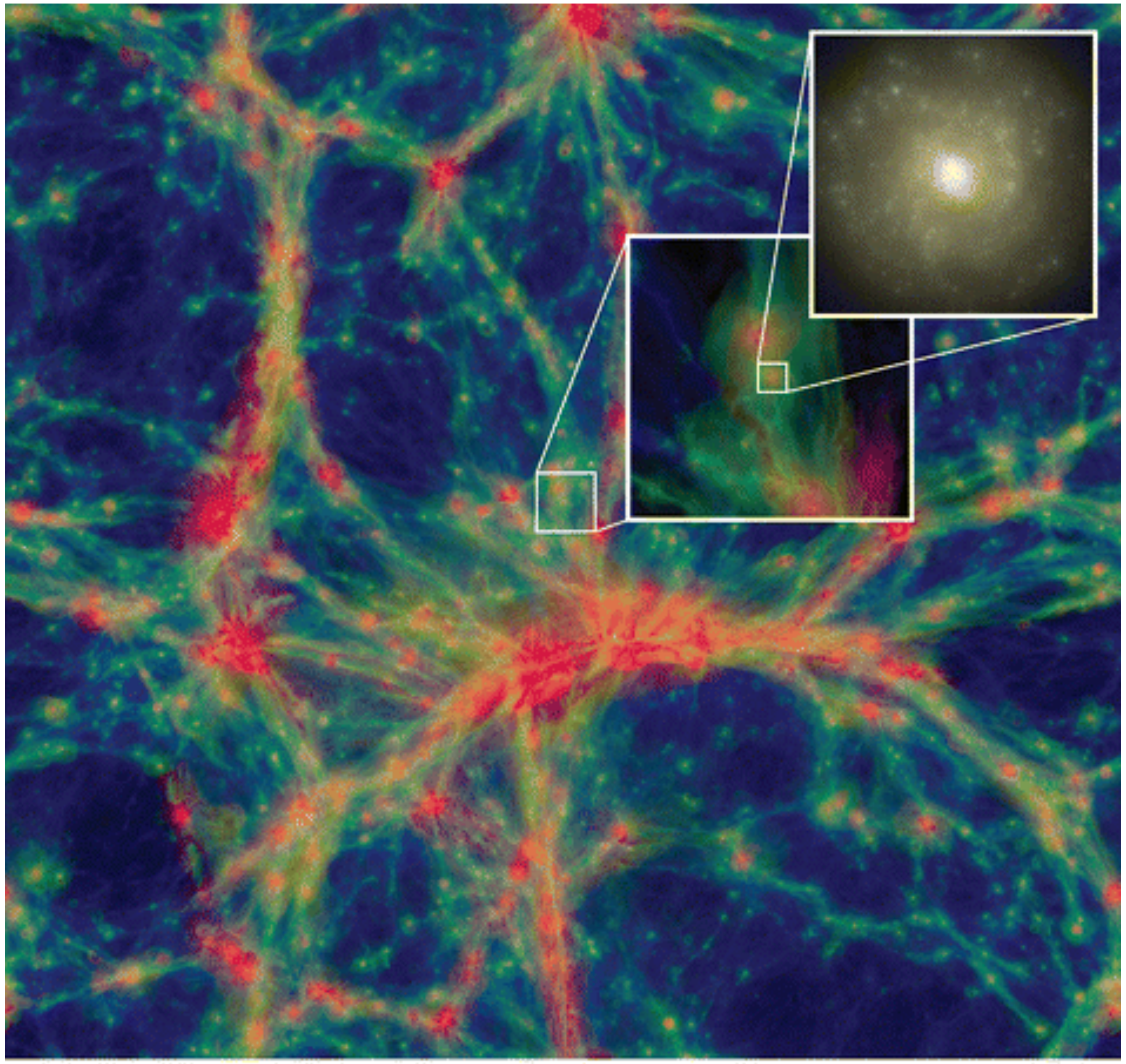

AR Somerville RS, Davé R. 2015.
Annu. Rev. Astron. Astrophys. 53:51–113

Current explanations for the various small scale problems generally invoke complicated "baryonic physics" in hydrodynamic cosmological simulations that include every effect but the kitchen sink.

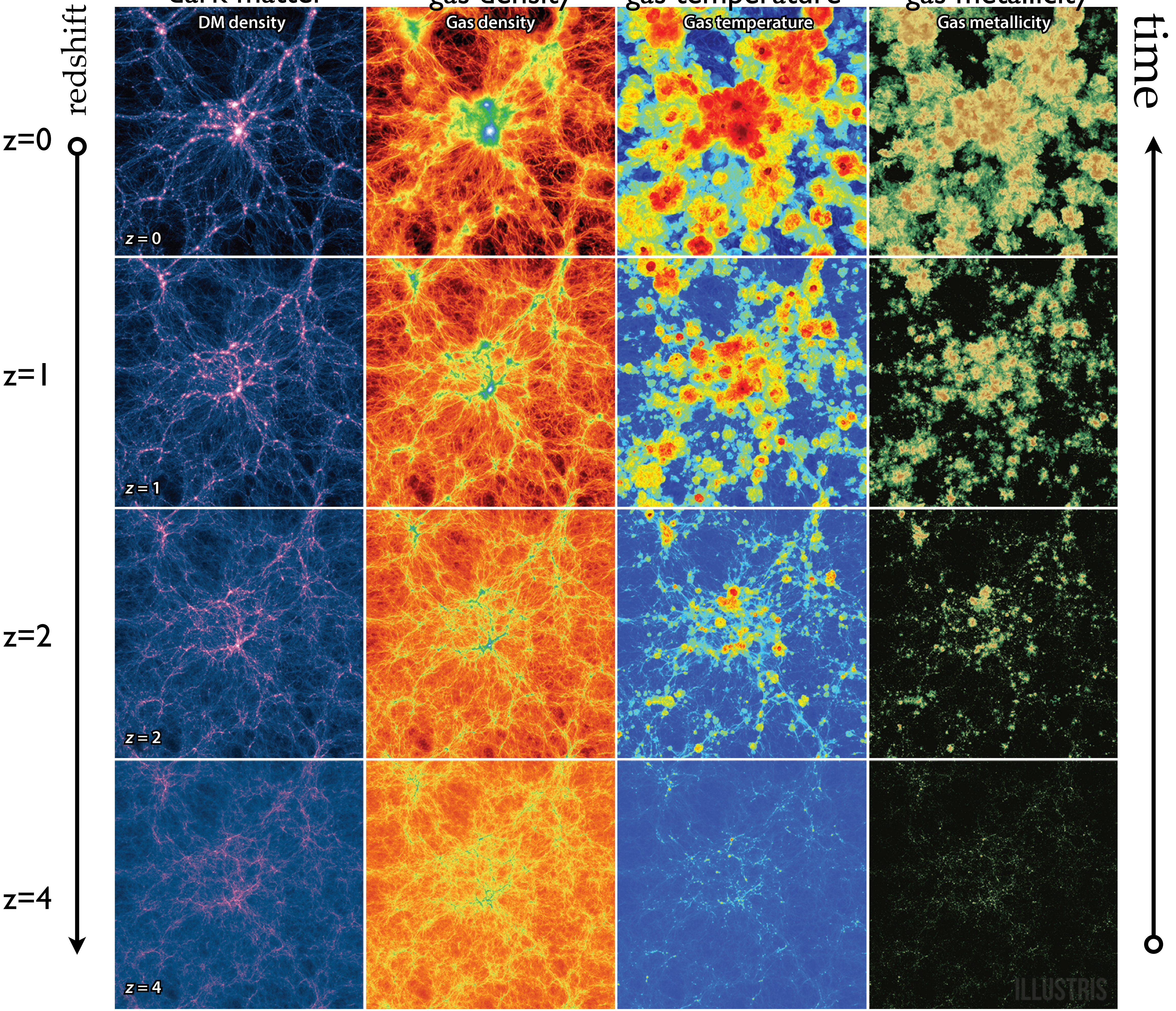

Illustris simulation

dark matter

gas density

gas temperature

gas metallicity

redshift

z=0

z=1

z=2

z=4

time

now

Halo assembly by mass

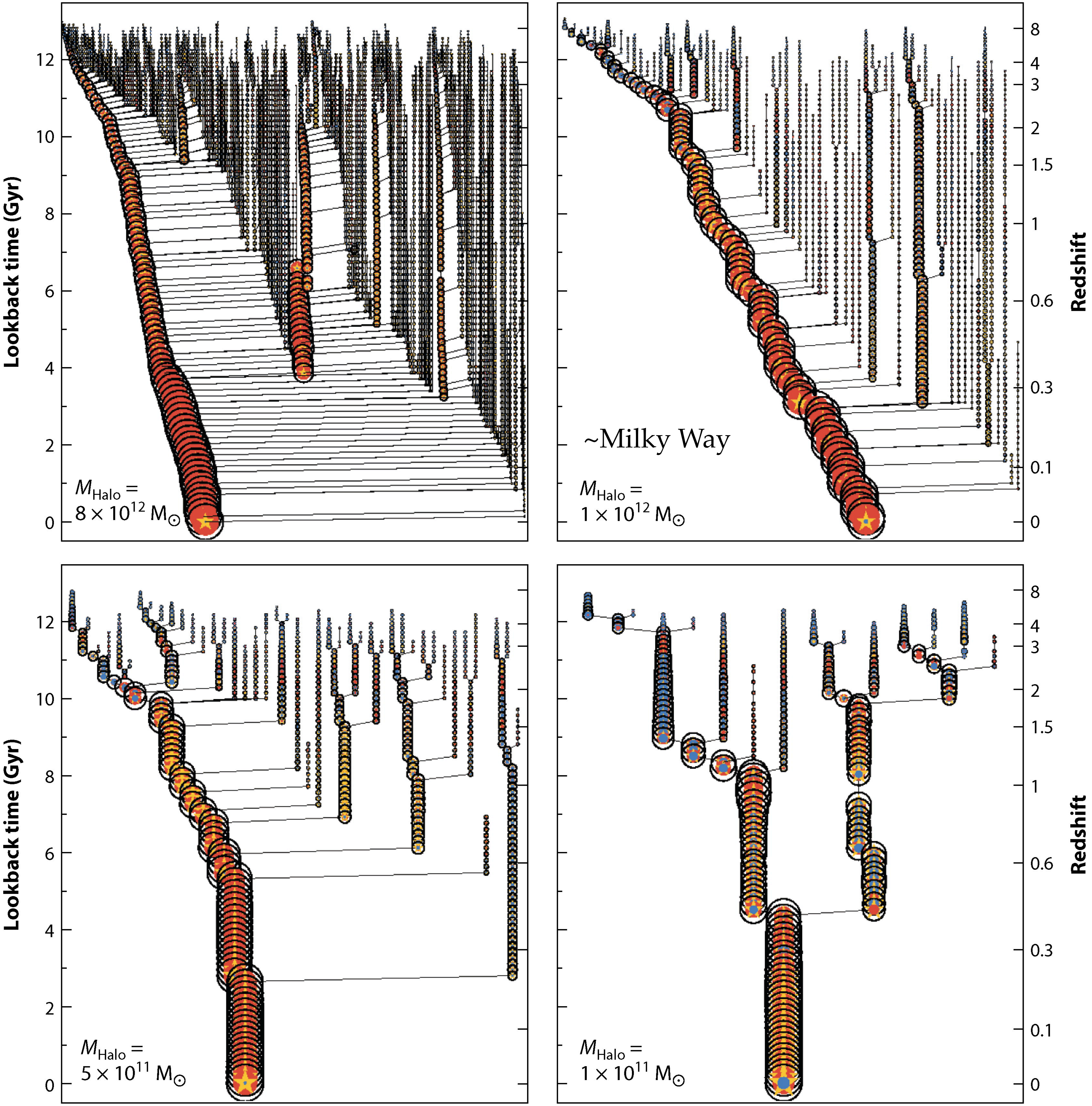

Stellar mass function

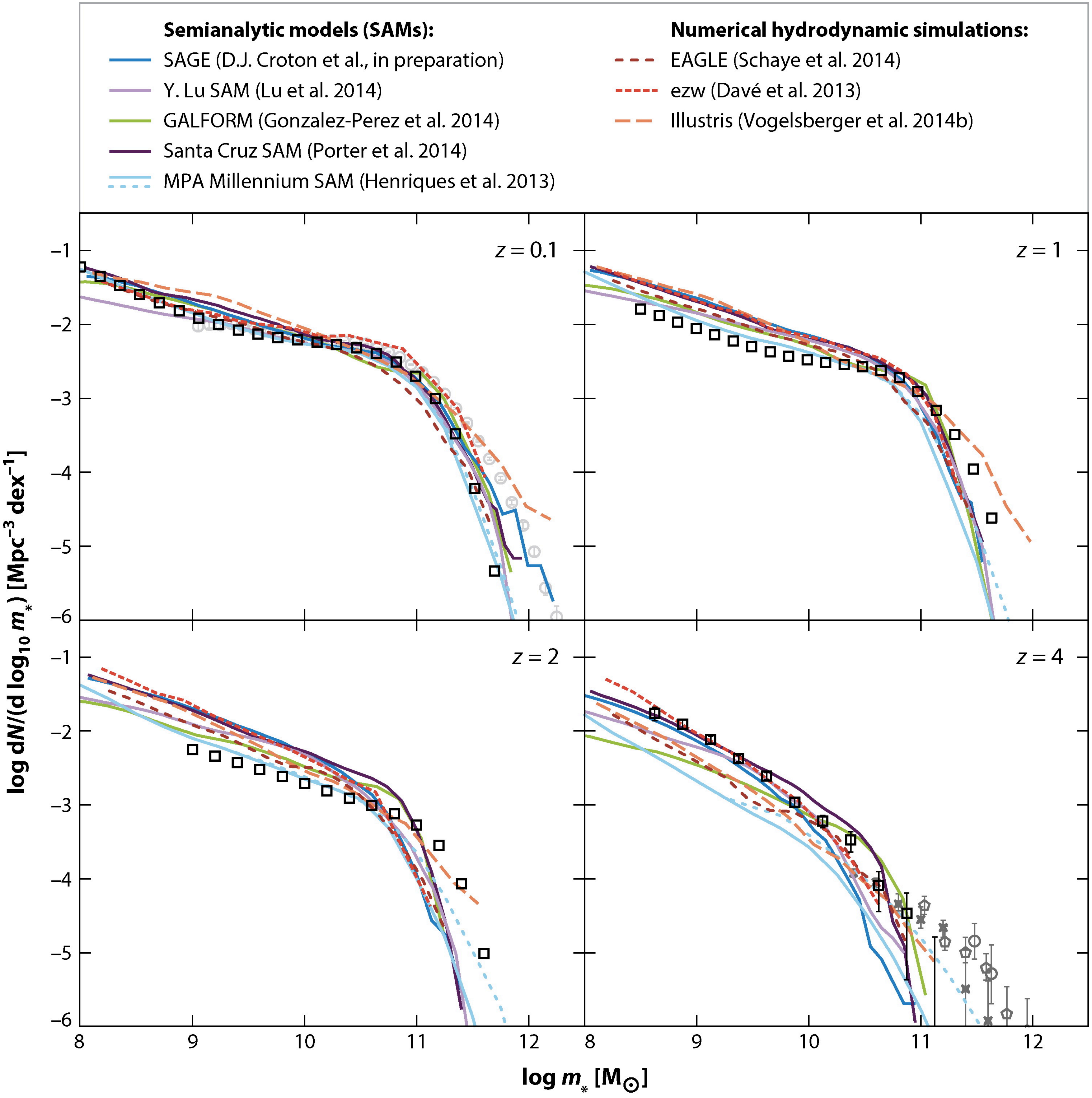

Bars

- Non-axis-symmetric potential
  - provides perturbing torque to orbits
- Transfer angular momentum
  - stars get outward kick
  - gas sinks toward center
- Interact with dark matter halo
  - live halos may encourage bar growth, but
  - dynamical friction slows bars

Closed orbits in the rotating frame of a bar

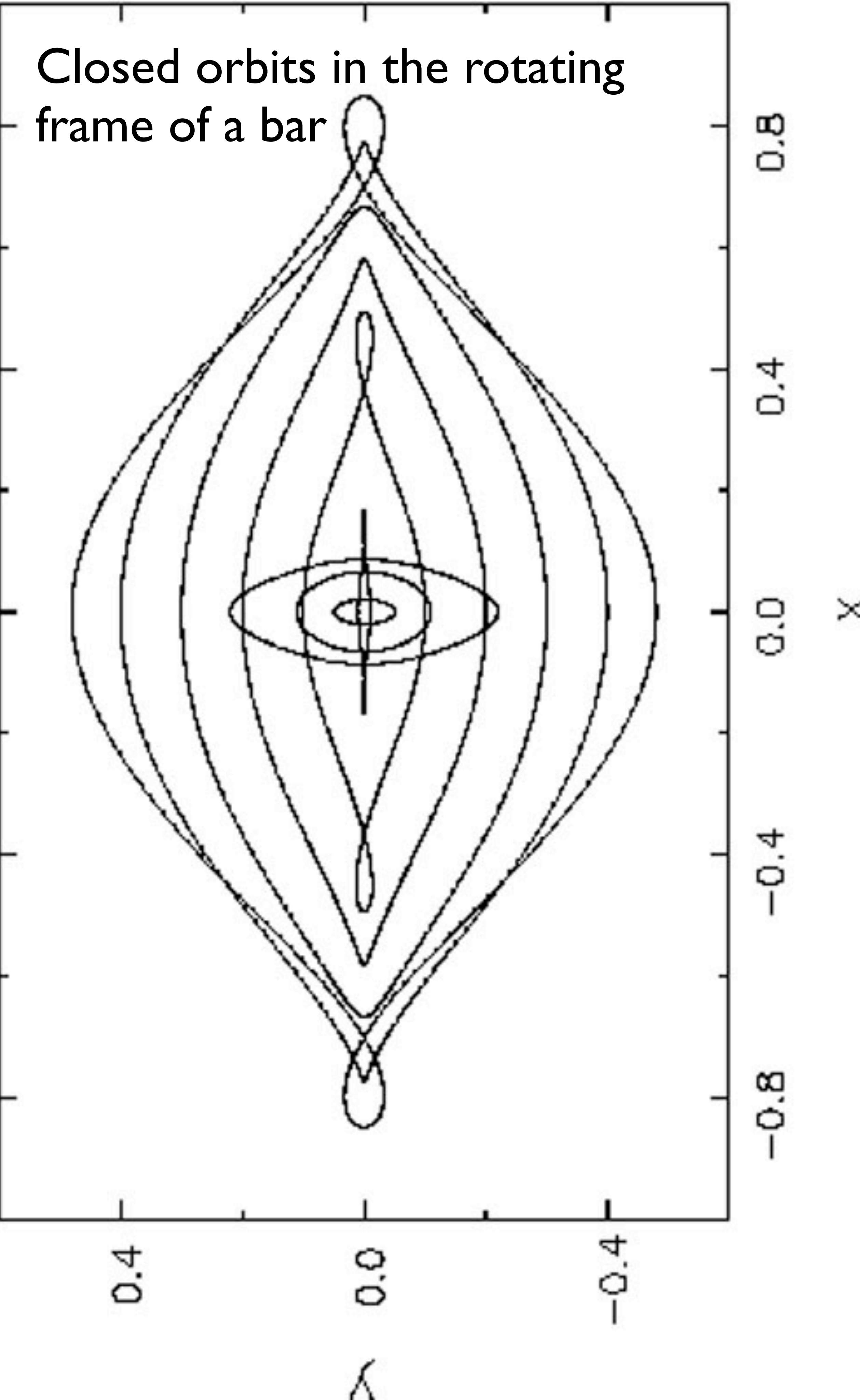

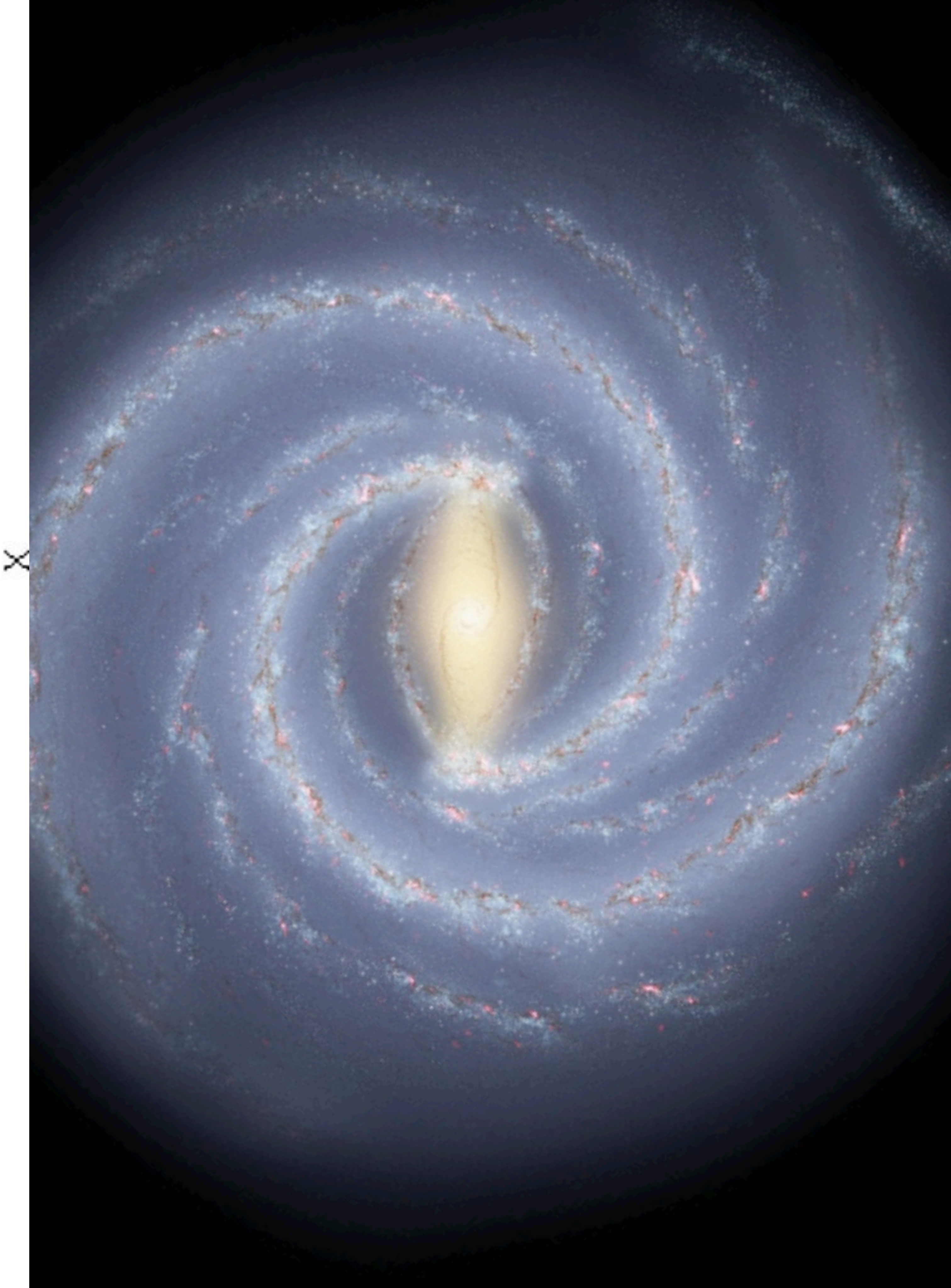

Lindblad resonances occur when

$$m(\Omega - \Omega_B) = \kappa$$

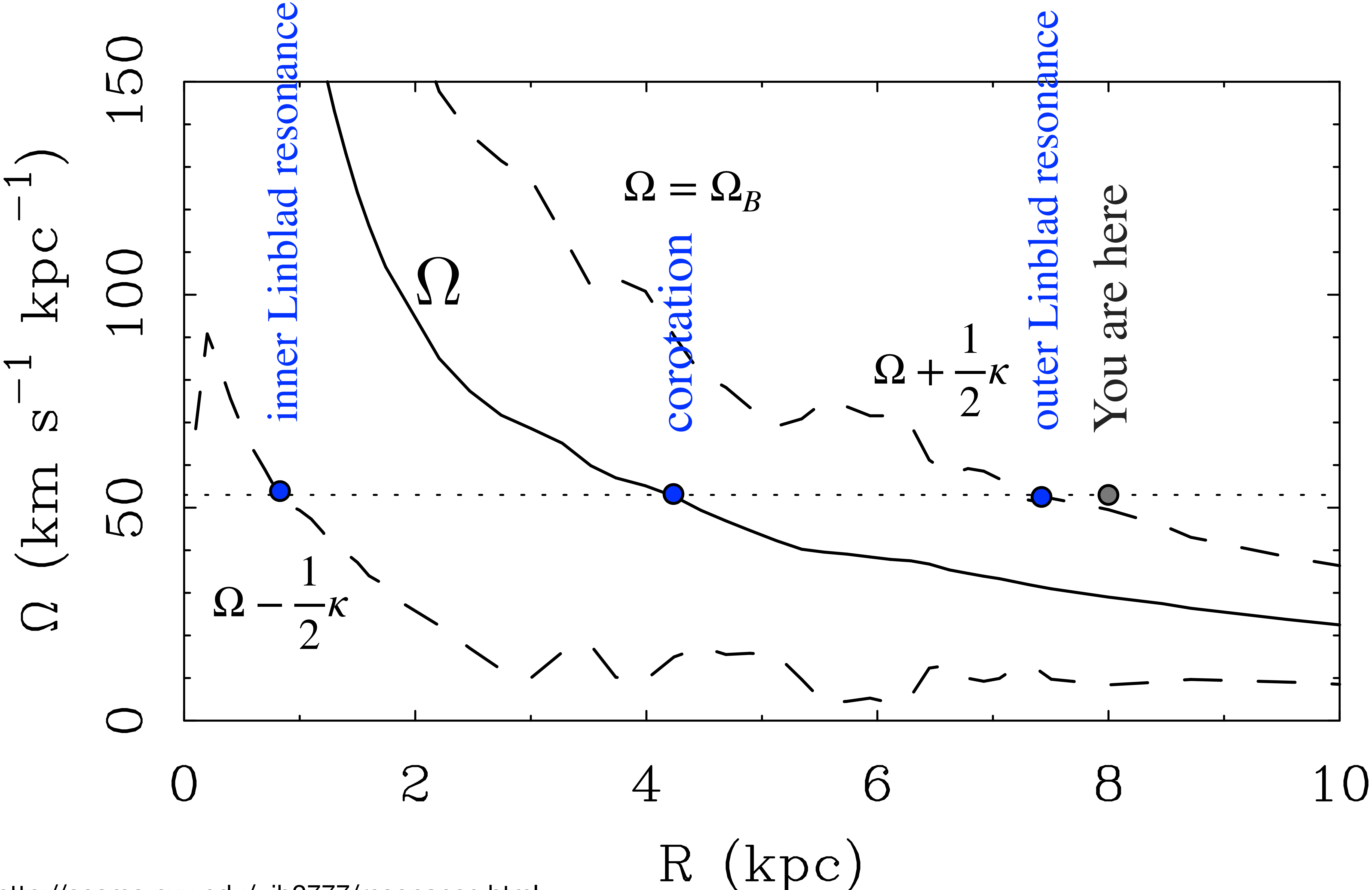

http://cosmo.nyu.edu/~jb2777/resonance.html

Bar lengths & measured bar pattern speeds

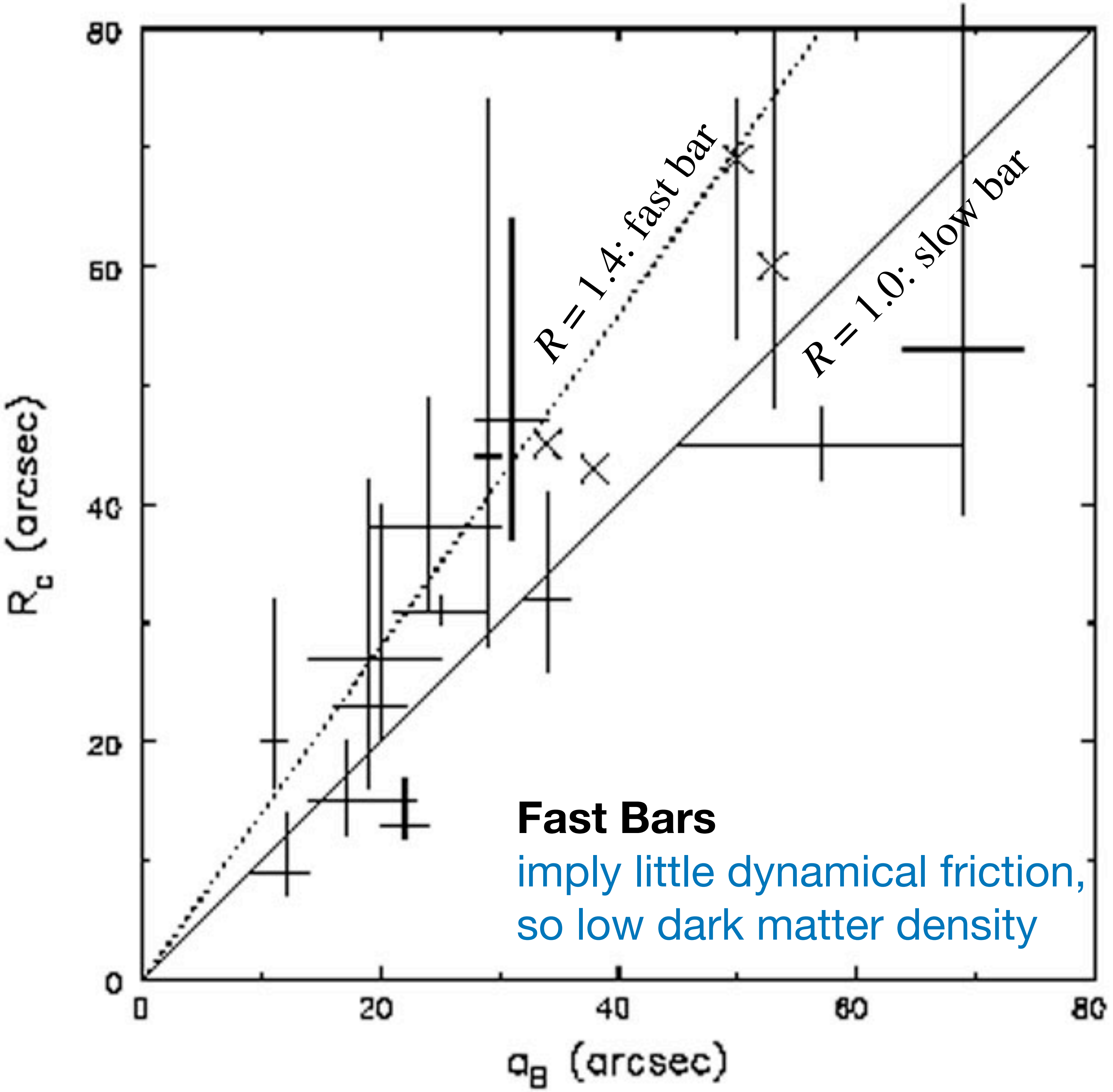

corotation radius

Fast Bars

imply little dynamical friction, so low dark matter density

bar length

Disk Stability

- Dark matter halos required for stability
  - No halo: bar instability
  - Too much halo: too stable - slow bars or no bars
- Spiral structure implies marginal stability
  - low modes least suppressed
  - Grand design (m=2) spiral pattern indicates substantial disk self-gravity
- Mergers destroy disks
  - limits mass ratio of mergers.
    - 1:1 Bad.   10:1 OK.

Spiral Structure

From swing amplification (Toomre 1981)

Growth of m=2 mode as it oscillates between the inner and outer Lindblad resonances

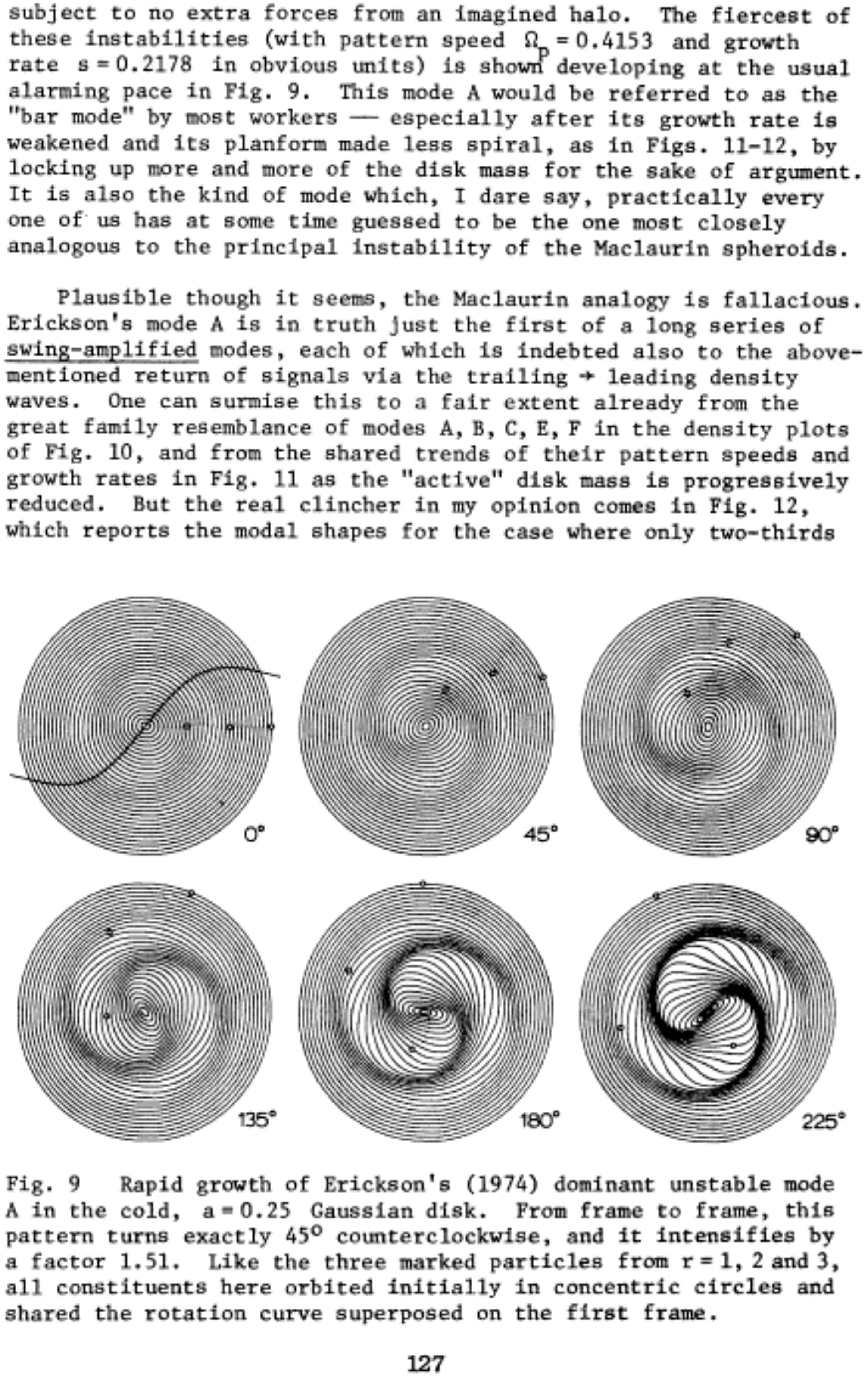

subject to no extra forces from an imagined halo. The fiercest of these instabilities (with pattern speed $\Omega_p = 0.4153$ and growth rate $s = 0.2178$ in obvious units) is shown developing at the usual alarming pace in Fig. 9. This mode A would be referred to as the "bar mode" by most workers — especially after its growth rate is weakened and its planform made less spiral, as in Figs. 11-12, by locking up more and more of the disk mass for the sake of argument. It is also the kind of mode which, I dare say, practically every one of us has at some time guessed to be the one most closely analogous to the principal instability of the Maclaurin spheroids.

Plausible though it seems, the Maclaurin analogy is fallacious. Erickson's mode A is in truth just the first of a long series of swing-amplified modes, each of which is indebted also to the above-mentioned return of signals via the trailing → leading density waves. One can surmise this to a fair extent already from the great family resemblance of modes A, B, C, E, F in the density plots of Fig. 10, and from the shared trends of their pattern speeds and growth rates in Fig. 11 as the "active" disk mass is progressively reduced. But the real clincher in my opinion comes in Fig. 12, which reports the modal shapes for the case where only two-thirds

Fig. 9 Rapid growth of Erickson's (1974) dominant unstable mode A in the cold, $a = 0.25$ Gaussian disk. From frame to frame, this pattern turns exactly 45° counterclockwise, and it intensifies by a factor 1.51. Like the three marked particles from $r = 1, 2$ and 3, all constituents here orbited initially in concentric circles and shared the rotation curve superposed on the first frame.

Athanassoula et al. (1987) pointed out that a minimum amount of disk self-gravity was required to drive spiral structure, providing a lower limit on the masses of spiral disks.

Too much disk mass: the disk is unstable.

Too little disk mass: the disk is too stable to sustain spiral structure.

should bracket the reality. We then obtain for each arm multiplicity an estimate of the range in radii over which amplification is permitted. The proper value of Q is not important (cf. Fig. 7 of Toomre, 1981 or Fig. 26 of Athanassoula, 1984. If the allowed $m = 1$ amplification is large we lower the $(M/L)_d$ as necessary. When a solution with no sizeable $m = 1$ is found we label it "maximum disk with $m = 1$ inhibited" or, for short, "no $m = 1$". The amplification drops sharply as the M/L is decreased (see Fig. 8 of Toomre 1981) so the range of M/L_d over which the transition from significant to no amplification occurs is relatively small. We then continue lowering the $(M/L)_d$. When we reach the point were the $m = 2$ amplification is in turn inhibited we

$\mathrm{MH}(R_{25}/3)/\mathrm{MH}(R_{25})$. Secondly, an isothermal sphere model is fitted to the halo velocities from which we obtain a core radius (R_c), central density (ρ_0), dispersion (σ), halo mass within R_{25} and concentration indices as above. The last fit is that of a power law to the halo density. All these quantities will be used later to parametrize the halo.

An illustration of the modelling has been reproduced in Fig. 1 for the galaxy NGC 598. Figure 1a shows the photometry data. The "maximum disk" solution is given in Fig. 1b by a solid line, together with the observed velocity data. The amplification factors for NGC 598 are plotted in Fig. 1d for both $m = 2$ and $m = 4$. For this galaxy the maximum disk solution has no $m = 1$

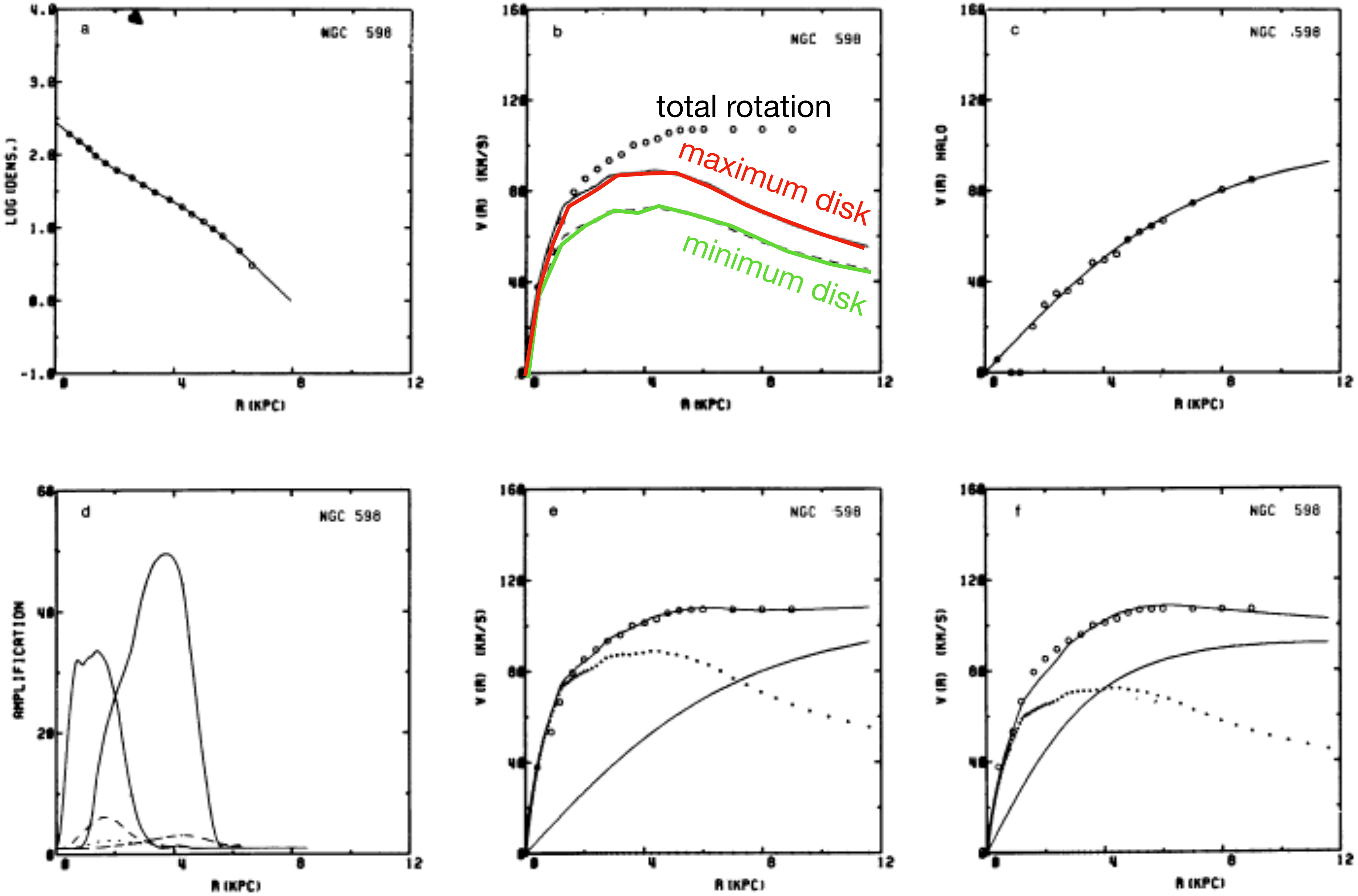

Fig. 1a–f. Mass model for M 33. **a** The radial luminosity profile taken from De Vaucouleurs (1959). **b** Rotation curves calculated for the maximum disk solution with M/L (corr) = 1.89 (solid curve), and the no $m = 2$ solution with M/L (color) = 1.24 (dashed curve). The observed rotation data (circles) have been taken from Newton (1979). **c** Isothermal sphere model fitted to the halo velocities obtained for the maximum disk solution. **d** Amplification factors as function of radius for the no $m = 1$ solution for $m = 2$ (left side) and $m = 4$ (right side). The curves are for different values of Q: 1.2 (solid lines), 1.5 (dashed lines), and 2.0 (dashed-dotted lines). **e** final composite for the no $m = 1$ solution. The disk curve, the isothermal halo fit, and the composite are shown, together with the observed data (circles). **f**, as e, but for the no $m = 2$ solution

Mergers thicken and heat disks. The existence of cold, thin disks (spiral galaxies) limits the mass of mergers to < 1:10 (crudely speaking).

Toth & Ostriker (1992)

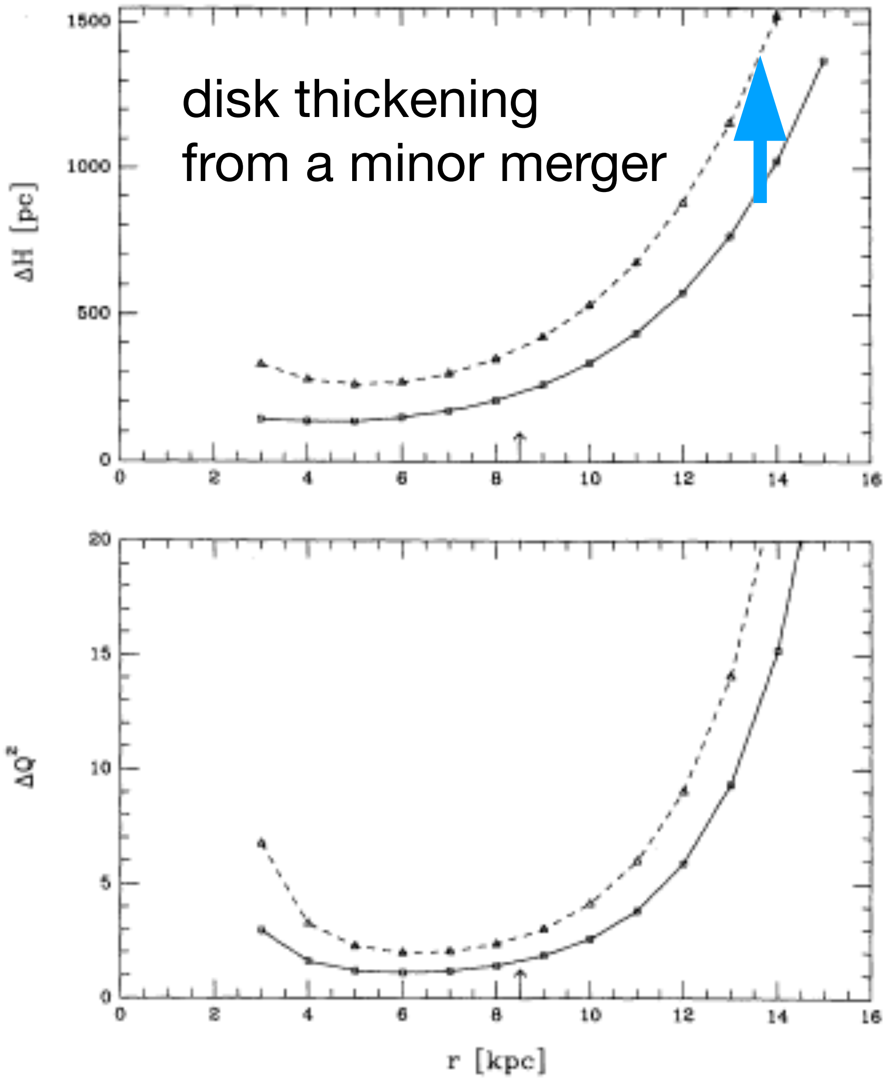
disk thickening from a minor merger

ght and Toomre's Q in the Caldwell-Ostriker galaxy model. The infalling satellites are modeled by Jaffe spheres with a total mass of
the solar circle ($=4.3 \times 10^9\ M_\odot$) and scale lengths of 1 kpc (*solid lines*) or 0.1 kpc (*dashed lines*). They are assumed to spiral in along
distribution of orientations. See § 4 for details. In the top panel the scale-height increase ΔH is plotted against the Galactocentric
ne change in Toomre's Q^2 is shown.

Odds of dodging a major merger are small…

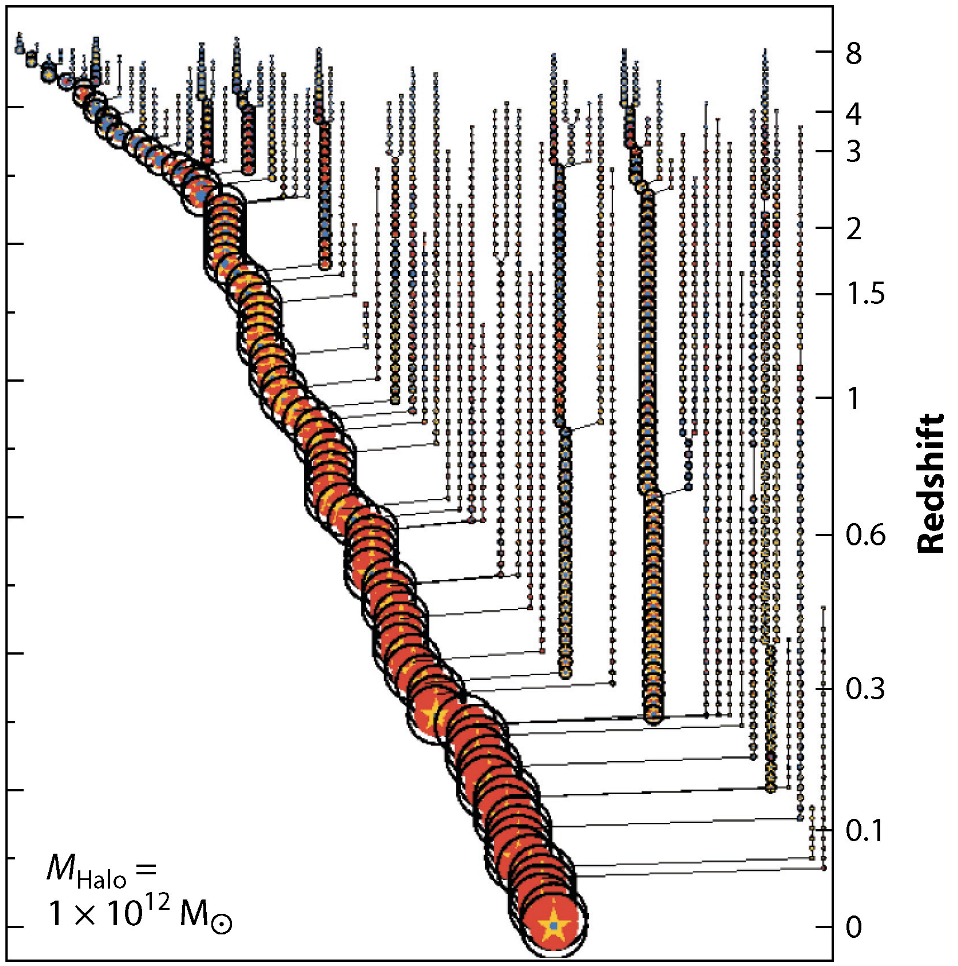

…but cosmology dependent.
How special is the Milky Way?

The Milky Way has an old (~9 Gyr) thick disk, that is a modest fraction of the total stellar disk mass. Perhaps a sizable merger thickened the disk long ago, but not much has happened since.

Thin disk
Age: 8 Gyr

Thick disk
Age: 9.5 Gyr
mass fraction: ~20%

Stellar Halo
Age: 12.5 Gyr
mass fraction ~1%

Ages from oldest white dwarfs
(Mukremin et al. 2017)

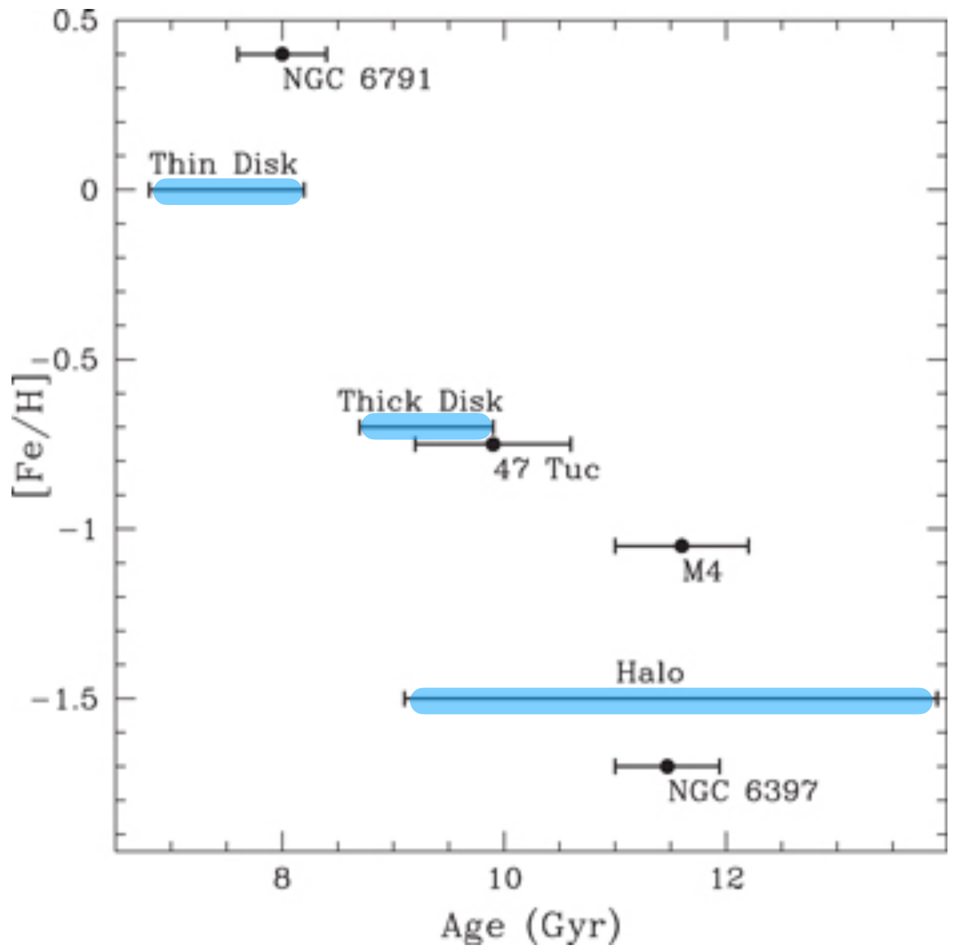

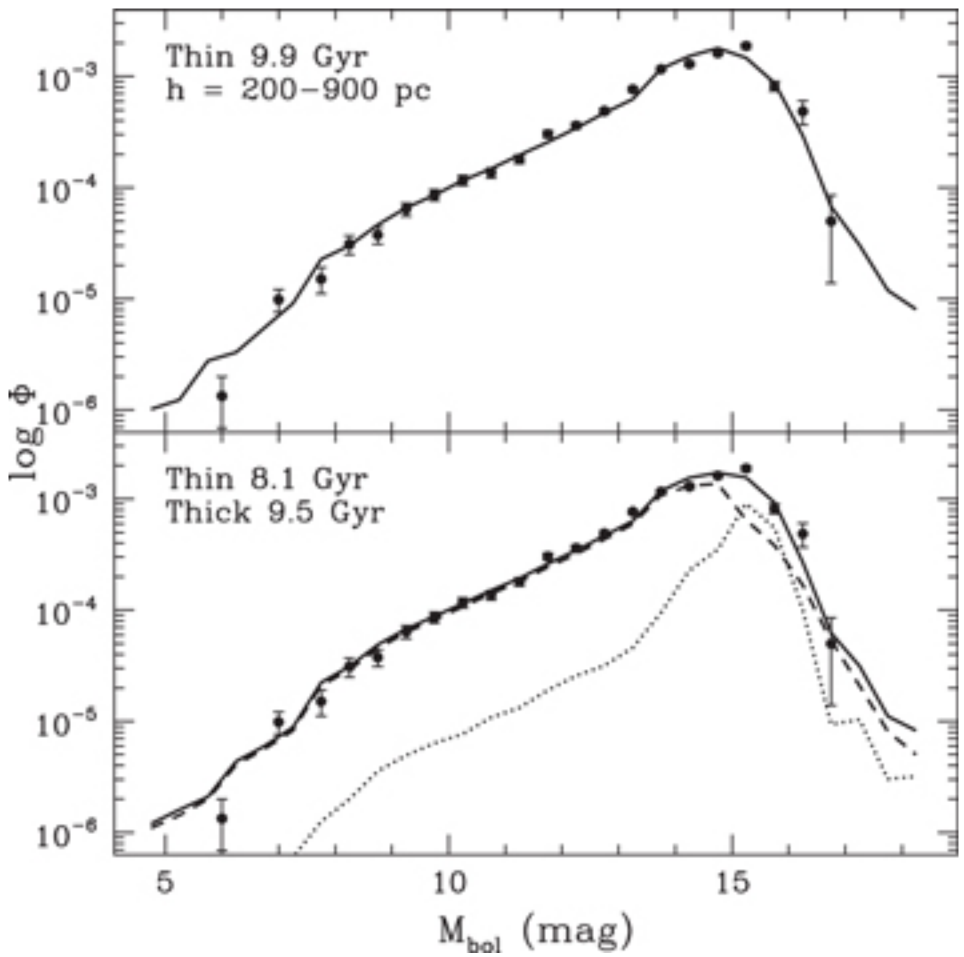

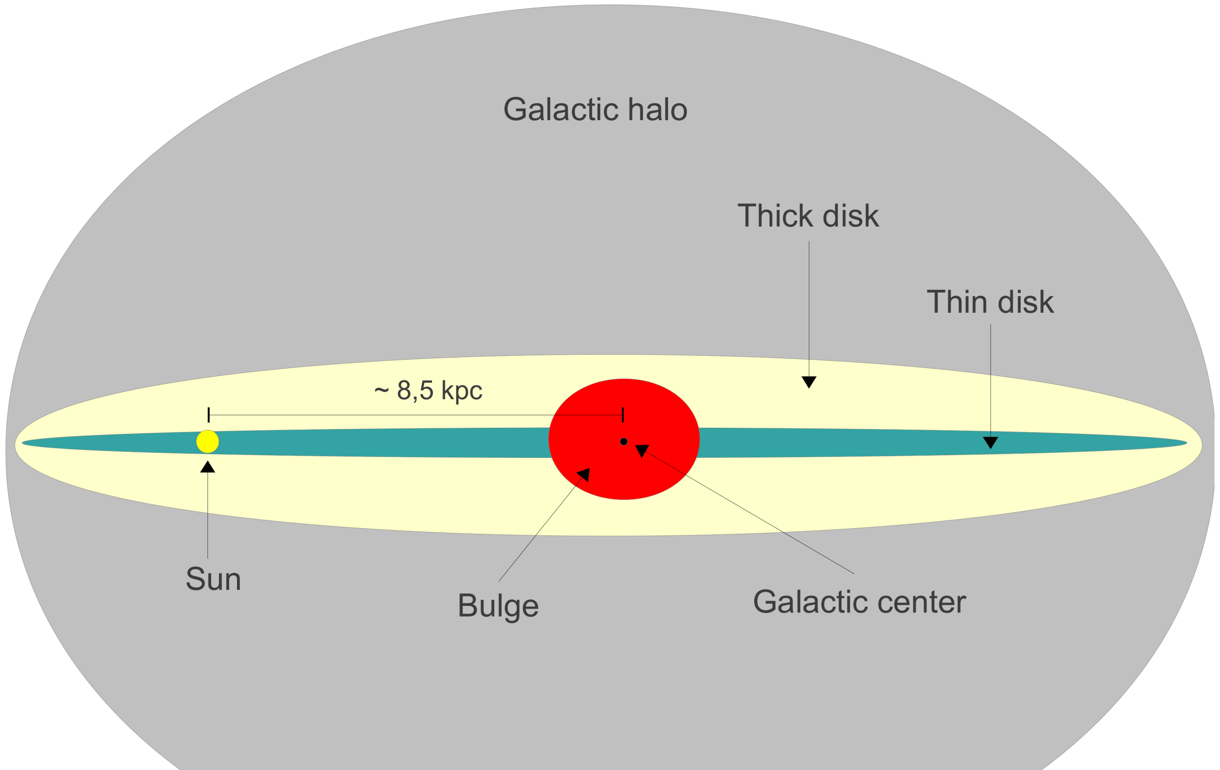

The Milky Way has an old (~9 Gyr) thick disk that is a modest fraction of the total stellar disk mass. Perhaps a sizable merger thickened the disk long ago, but not much has happened since.

Dynamical friction acts to slow a particle of mass M and velocity v_M traversing a medium of N gravitationally attractive particles each of mass m.

consider a mass, M, moving through a uniform sea of stars. Stars in the wake are displaced inward.

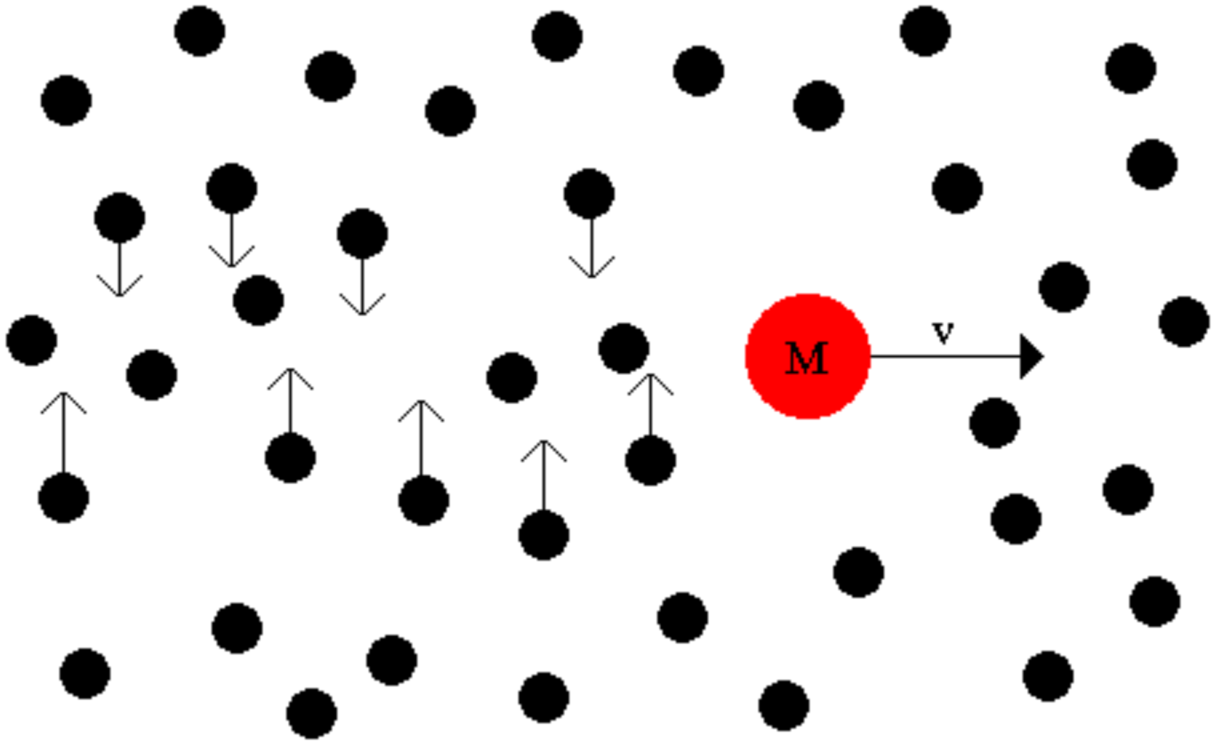

Dynamical friction arises when the passage of an object pulls particles towards it, creating a density enhancement in its wake. This density enhancement pulls back against the motion of the object.

this results in an enhanced region of density behind the mass, with a drag force, F_d known as dynamical friction

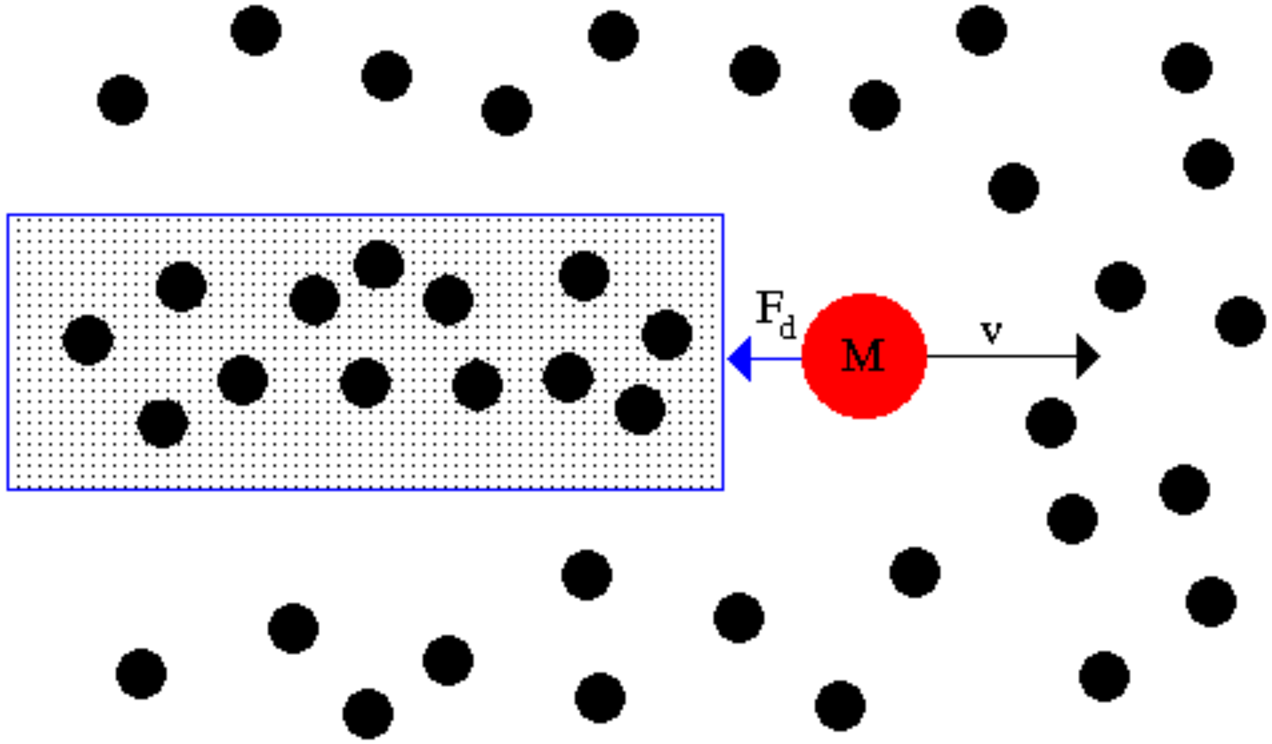

Dynamical friction acts to slow a particle of mass M and velocity v_M traversing a medium of N gravitationally attractive particles each of mass m.

Chandrasekhar formula for dynamical friction (BT eqn 8.3)

$$\frac{d\vec{v_M}}{dt} = -16\pi^2 G^2 M m \ln\Lambda \frac{\vec{v_M}}{v_M^3} \int_0^{v_M} f(v) v^2 dv$$

net frictional force

Coulomb logarithm

distribution fcn of background particles (N of mass m and velocity v)

The Coulomb logarithm measures the “extent” of the system and is a complete kludge

$$\Lambda \approx \frac{b_{max}}{b_{min}} \approx \frac{NmR}{M\mathcal{R}}$$

orbital radius of mass M

extent of N masses m

e.g., the radius of a dark matter halo

Examples where dynamical friction is important

- Dynamical friction acts to slow the pattern speed of bars embedded in dark matter halos.

Mostly. We think. Some configurations of live halos can amplify rather than suppress bars!

- Plays a role in the orbits of satellite galaxies and their incorporation into larger dark matter halos.

- Also required for merging galaxies - orbital energy and angular momentum gets transferred to the dark matter halo, which acts like a big catchers mitt to make galaxies merge that would otherwise just fly past each other.

The Antennae [merger of NGC 4038 and NGC 4039]

Merging galaxies simulation by Prof. Mihos

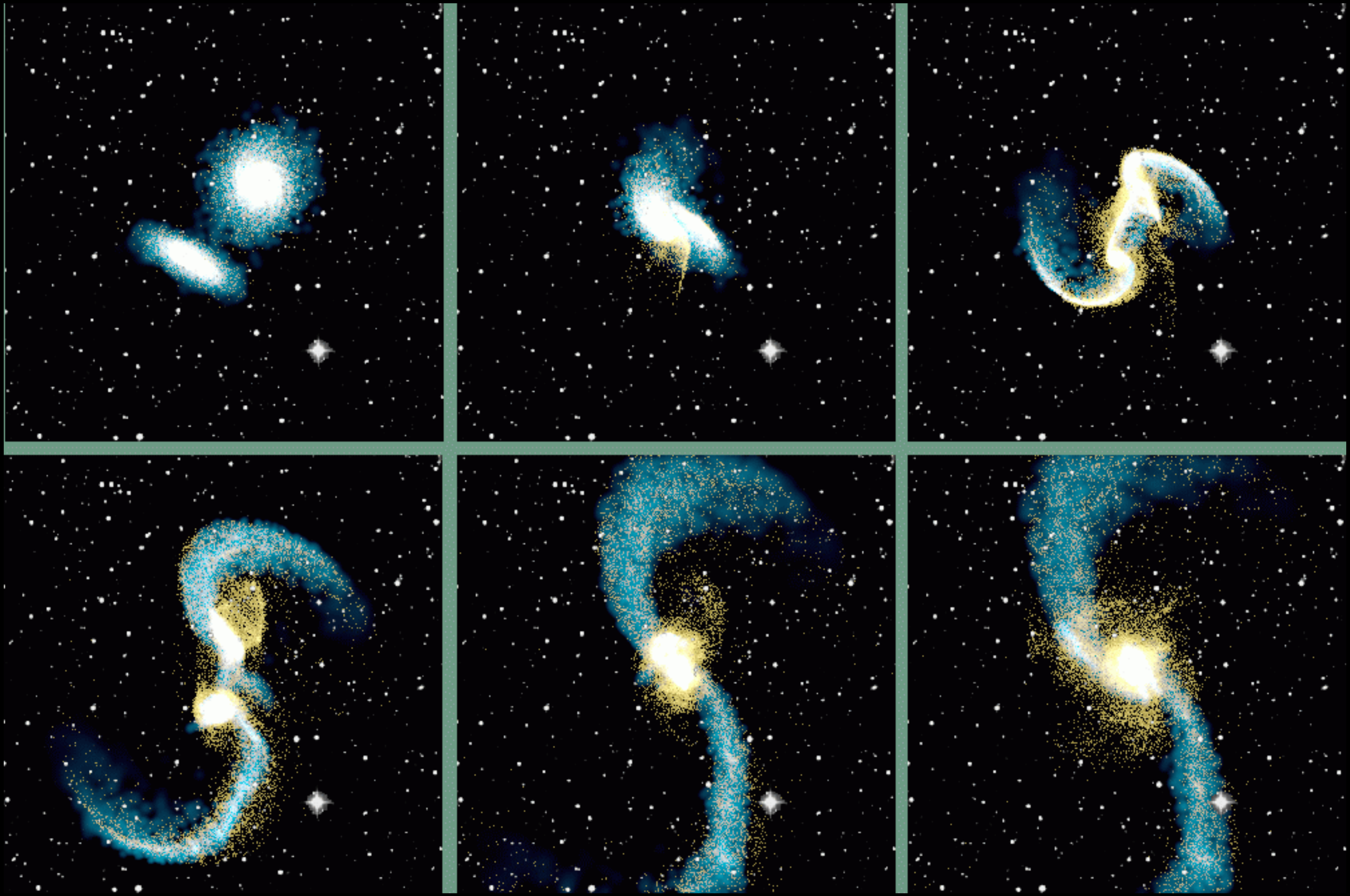

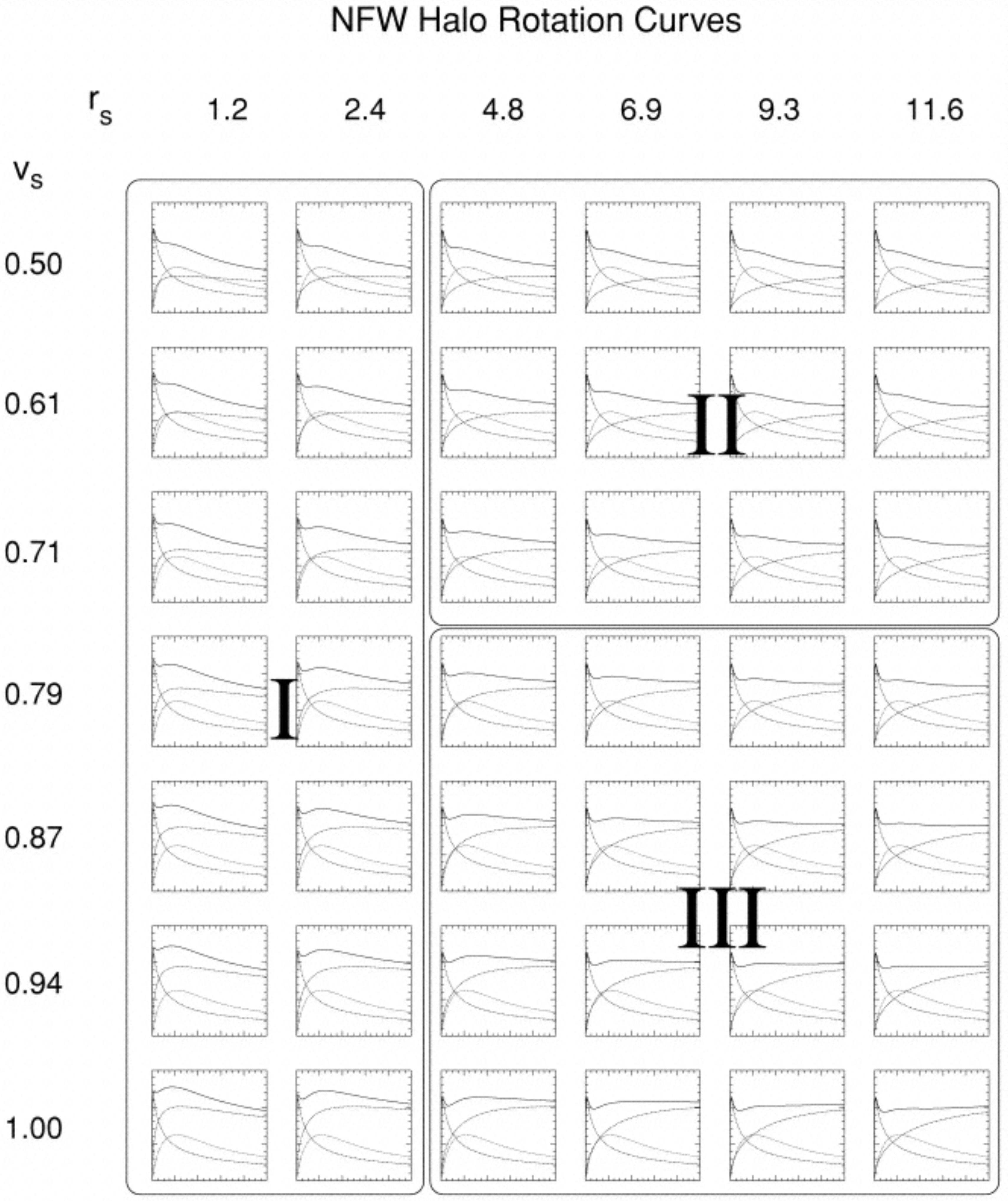

Merging galaxy models
initial rotation curves

Dubinski, Mihos & Hernquist (1999)

Zone II gives the most realistic tidal tail morphologies.

Zone III has more realistic rotation curves.

small contradiction, that.

The potential well of the DM halo needs to be deep enough to cause a merger, but not so deep that it inhibits the formation of tidal tails.

Merging galaxy models

morphology of merger models

Dubinski, Mihos & Hernquist (1999)

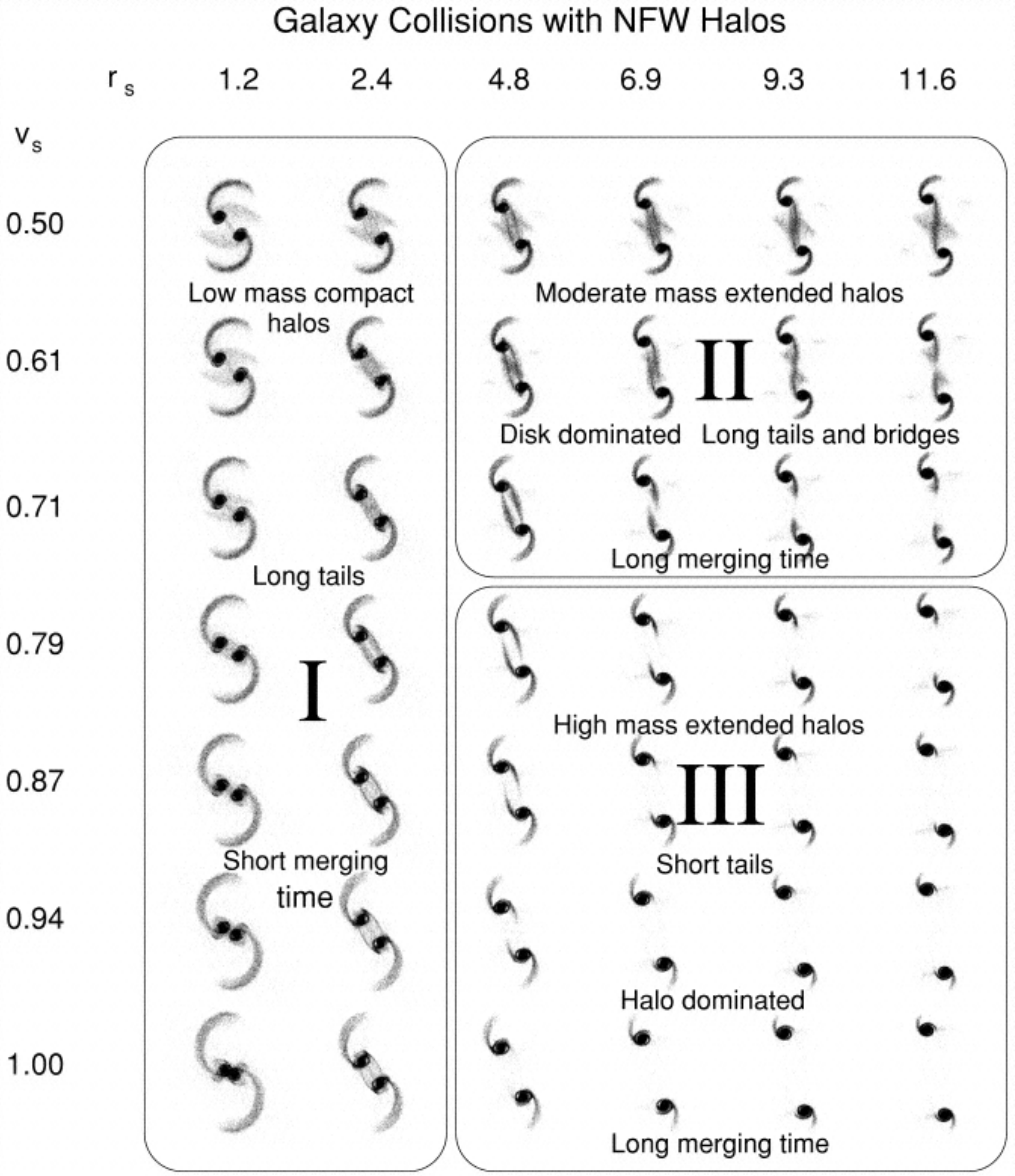

Zone II gives the most realistic tidal tail morphologies.

Zone III has more realistic rotation curves.

small contradiction, that.

The potential well of the DM halo needs to be deep enough to cause a merger, but not so deep that it inhibits the formation of tidal tails.